

Estimating Subsurface Permeability with 3D Seismic Attributes: A Neural Net Approach

John Casteel

Agua Caliente, LLC

Satish Pullammanappallil

Optim, Inc

Robert J. Mellors

Lawrence Livermore National Laboratory, Livermore, CA, 94155, USA

e-mail: mellors1@llnl.gov

Keywords: permeability, reflection seismic, attributes

ABSTRACT

We seek to map subsurface permeability in a geothermal area using 3D seismic attributes extracted from a 14 square mile 3D seismic reflection survey acquired over the Walker Ranch geothermal prospect at Raft River, Idaho. A set of attributes was estimated and a neural net approach used to infer relationships between the attributes and permeability index, as well as other information including resistivity and lithology. The analysis was conducted two ways: using commercial software and an independently developed code. Several types of neural net algorithms were tested. A training set was constructed using an estimated permeability index derived from well data. Several ways of parameterizing the observed permeability distribution inferred from the well data were tested. Validation was conducted using a 'leave one out' strategy. The neural net was successful in determining relationships between the training set and the attributes at a high correlation level but results from the validation were inconsistent due largely to problems with false positives. The 3D seismic data was also used to examine the locations of known microseismic events with respect to features in the depth migrated 3D reflection data. Only a general correspondence between the microseismic hypocenters and observed faults in the 3D seismic volume was observed, with no direct relationship with a clearly imaged fault.

1. INTRODUCTION

The primary goal in geothermal exploration is to find a location with high temperatures and sufficient flow rate to allow for economic recovery of the heat. While elevated temperatures in the sub-surface are not uncommon, the high permeability and flow rate required for economic prospect is more rare. In addition, measuring permeability at depth is difficult without drilling. Unfortunately, drilling is expensive and time-consuming and often several wells may be necessary to adequately delineate a field. Therefore, finding a cost-effective method of estimating permeability at depth using geophysics would reduce costs of exploration and reduce risk, leading to lower costs of produced power and additional prospects.

Seismic reflection is a geophysical tool that is frequently used in petroleum exploration. Its use in geothermal exploration is less standard, in part due to relative cost and the challenges in identifying the highly-permeable zones essential for economic hydrothermal systems (e.g. Louie et al., 2011; Majer, 2003). Newer technology, such as wireless sensors and low-cost high performance computing, has helped reduce the cost and effort needed to conduct 3D surveys. Currently the cost is much less than that of a drilling campaign. The second problem of identifying permeable zone is more difficult. In this work we test the use of seismic attributes from a 3D seismic survey to identify and map permeable zones in a producing hydrothermal area.

Unfortunately, seismic wave propagation is largely insensitive to temperature or permeability directly. In general, fractures are expected to decrease velocities and increase attenuation (Nakagone et al., 1998). Alteration may also decrease velocities (Unruh et al., 2001) while mineralization associated with water flow may increase velocities (Majer, 2003). Standard seismic interpretation uses the seismic amplitudes as a function of time (or depth) to image sub-surface features such as faults or dramatic changes in lithology. The resolution of seismic surveys is much larger than the fracture size and therefore individual fractures cannot be imaged directly in most cases. A more advanced technique uses alternate characteristics (attributes) of the seismic traces to infer the existence of fractures below standard resolution. Considerable work in this area has been conducted by the petroleum industry in refining this type of analysis (Barnes, 1999; Barnes 2006, Chopra and Marfurt, 2007, Marfurt et al., 1998) and it has been used successfully for fracture detection (e.g. Neves et al., 2004) and in improving the success rate for petroleum detection.

Here our specific objective is to develop a process to reduce the risk associated with drilling additional production wells by attempting to directly image permeability and areas of high flow by using seismic attributes. As a test-bed, we will use a dataset of 3D seismic reflection data and ancillary well data from the Walker Ranch (adjacent to Raft River) geothermal area, Idaho. In this paper we refer to the producing geothermal area as Raft River and the adjacent area, which is the focus of this investigation, as Walker Ranch. As we are primarily focused on testing the concept in general, proprietary details specific to the Walker Ranch prospect (e.g. exact locations of cross-sections) that are not relevant to the overall process flow will be omitted.

The Raft River/Walker Ranch area has been the site of geothermal investigation since 1974. It is located in southern Idaho and is a large, moderate temperature resource (135-146 C) that produces from fractures near the interface of fractured Precambrian basement, faulted metamorphic layers and overlying Tertiary sediments (e.g. Jones et al., 2011; en.openei.org, 2015; Figure 1). High flow rates from basement rocks indicate significant fracturing. In particular the Narrows zone (Figure 1) and Bridge fault that extends to the north, are thought to provide structural control on the hydrothermal area. Based on geochemical and resistivity data, the Narrows zone appears to divide the hydrothermal area into two compartments and may be an impermeable basement shear zone. Recharge appears to be both lateral and horizontal. Current production from Raft River is about 11 Mw from four production wells. The area is currently the site of an enhanced geothermal system demonstration project (Bradford et al., 2015). Micro-seismicity does occur near the areas of geothermal production, however primarily along a line of injection wells, within the Narrows zone in the Precambrian basement.

The 3D dataset from Walker Ranch was acquired and processed by Optim, Inc. under contract to Agua Caliente. An area of approximately 14 square miles was covered in two surveys (Figure 1), with a crossline spacing of 660 feet and inline of 165 feet using a Vibroseis source. Processing included depth migration. The 3D seismic dataset was extensively mapped manually for horizons and faults and all available well data included and tied. While data quality was good, the geology and complexity of the region did not lend itself to simple interpretation. The upper section did not display clear horizons and while the basement interface (quartzites and schist under the Tertiary Salt Lake formation sediments) created high amplitude reflections in some places, the reflections tended to be discontinuous. Faults, while clearly present, were difficult to map, even with the aid of commonly used attributes to assist interpretation. The Narrows zone is not a clear and distinct feature in the 3D seismic volume, however structural element that correlate with MEQ locations are visible.

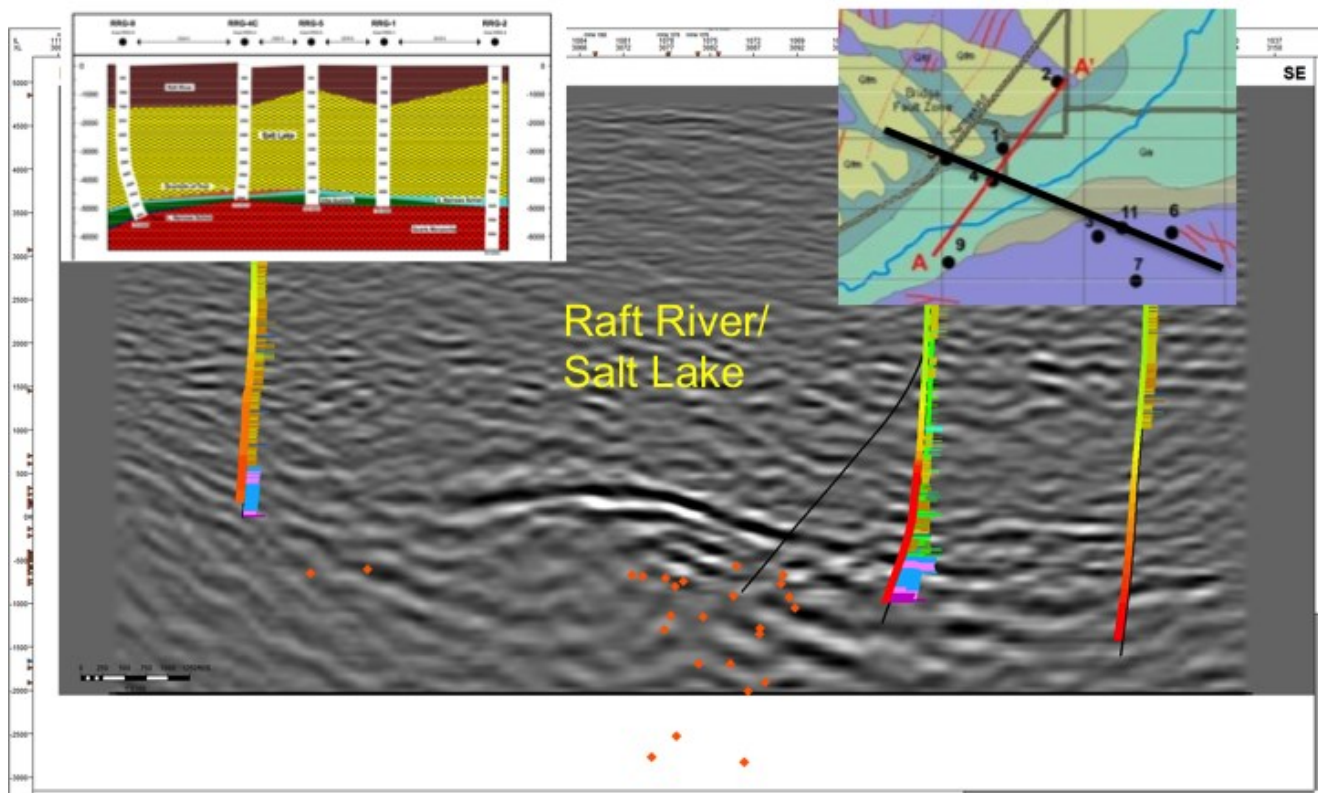


Figure 1: Cross-section of Walker Ranch seismic data with geological cross at upper left and map showing location of seismic section (black line) and geological cross section (red line). Note that the geological cross section and the seismic section are roughly perpendicular to each other. Colored line are well tracks and orange dots are micro-earthquakes.

2. METHOD

As stated above, the goal is to image permeable zone using attributes and combinations of attributes. The analysis tasks were undertaken by Optim, Inc, and Agua Caliente using similar, but separate approaches. Optim developed in-house software while Agua Caliente used Petrel, a commercial seismic reflection interpretation program. The advantage of self-developed software is that algorithm details are known and adaptable. Commercial software provides ease of use but the exact details of internal functions may be proprietary. Results from both were compared.

The first step is to generate a set of seismic attributes. A wide number of attribute exist, and can be roughly classified into single trace and multiple trace attributes. Single trace attributes extract a feature of a one trace such as instantaneous frequency. Multiple trace attributes compare vales between adjacent traces. Coherency, which measures the similarity between neighboring traces, is an example of a multi-trace attribute. Due to the varying structure and discontinuous horizons, multi-trace attributes (similarity, curvature) yielded poor results in general.

Once the attributes are generated, the goal is to find an attribute, or combination of attributes algorithm that correlate with permeability. While it is possible to conduct this search manually, a more robust and unbiased method is to automatically search through attributes. A neural net approach was used, which is a machine learning algorithm originally designed to mimic biological systems. Typically, neural nets are “trained” on a dataset with known answers using some parameter as input. In this case, the seismic attributes are the primary ‘input’ and the desired output is the combination of attributes that identifies areas of high permeability. In addition to seismic attributes, mineralogical, lithological, and structural data were included. We were also careful to consider the attribute in terms of the underlying rock physics to ensure reasonable relationships.

Neural net analysis is conducted in two stages. First, a set of ‘training data’ is constructed that contains the input data (attributes) and a set of known desired results. In this case the attributes have been generated and a set of known permeability values taken from the well data were selected. The training set is used to determine the calibration for the neural net. It is often useful to reserve some known permeability values to serve as a validation sets later although this reduces the size of the training set. Second, once the neural net has been calibrated on the training data and evaluated, it is then applied to the full data set. In this case the training was conducted on values extracted near the well bore and then applied to the entire dataset. Ideally, this will reveal pockets of permeability in the data, which can be designated as potential drilling targets.

For the training set, permeability index values were extracted from three wells drilled by Agua Caliente at Walker Ranch. In order to accommodate variations in permeability along the wellbore, eight classifications of permeability were defined. These can be divided into two major categories: Type I and Type II. Type II classified points along the well either as “permeable” or “zero permeability”. Type I classified them as “permeable” and “undefined”. Type II is more rigorous but forces the algorithm to match sharp variations. Type I allows more gradual fitting. Selection of the proper permeability parameterization remains a challenge, as it has a strong influence on the results.

A comprehensive set of tests and preparatory runs were conducted prior to the final analysis. Initially, a variety of neural net algorithms were tested on a subset of the data and using only seismic attributes. During this stage the importance of carefully defining permeability became clear. Once a set of attributes was chosen, this set was used for a set of four models using a variety of permeability definitions and different input data sets. Some attributes performed well and matched the expected geology (Figure 2). In addition to seismic attributes, other geological and geophysical constraints were tested. A preliminary study was done to evaluate the use of attributes to identify the zone of microseismicity.

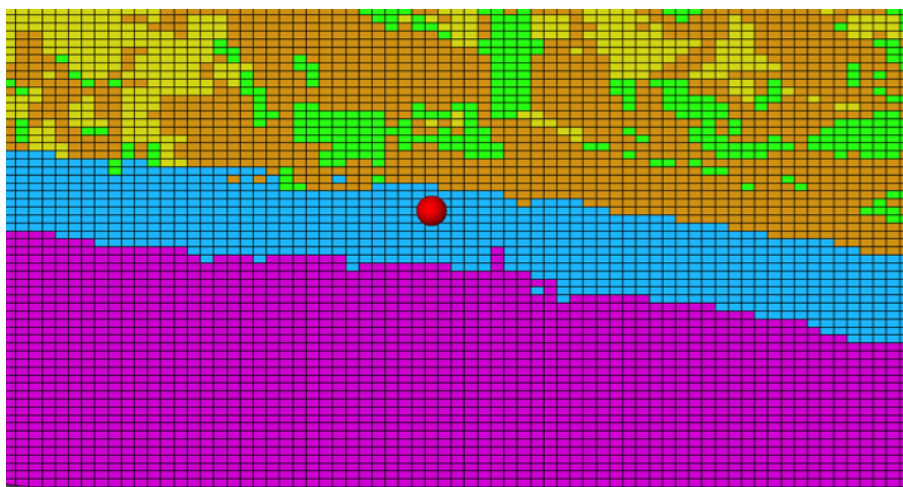


Figure 2: Vertical inline section through Facies Classification Attribute (Blue is Elba Quartzite, Green/Brown are Tertiary, Purple is Quartz Monzonite). Red dot shows location of measured high permeability in Elba Quartzite

2.1.1 Neural net algorithms

Four different neural net approaches were tested on 11 attributes derived from the 3D data. The shallow subsurface (upper 1900 feet) was excluded from the search. The input attribute file consisted of 2.2 million points and the permeability index (PI) file contained 2,069 points. Validation was accomplished by “leave one out”, i.e. known permeability index values that were not used in the neural net analysis were predicted based on the attributes. The four approaches were feed forward neural network with resilient back propagation (Reedmilller and Braun, 1993; Brieman, 1996); generalized regression with Gaussian layer (Specht, 1991), radial basis functions with Gaussian functions (Broomhead and Lowe, 1988), and support vector machine with Gaussian kernel (1997). The support vector machine algorithm was the fastest and most efficient. The results were mixed. In the first result the correlation between the expected and observed values was 0.78 with a standard error of 0.25, which is not very good. After smoothing the input attributes, the correlation increased to 0.95 with a standard error 0.11 (Figure 3,4). Analysis suggested that the observed permeability index values varied greatly over short spatial distances, which made fitting to more smoothly varying attributes difficult. In parallel, the neural net algorithm as implemented by the commercial software Petrel was tested. This allowed a greater range of input attributes although the details of the algorithm are not as precisely known.

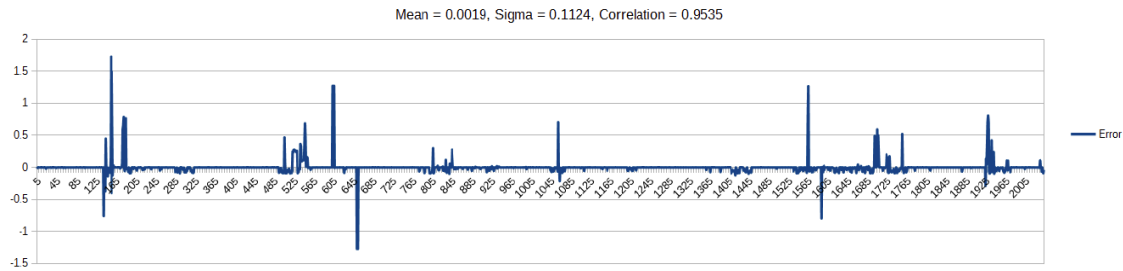


Figure 3: Plot of the difference between observed and predicted permeability index values using the ‘leave one out’ cross-validation. Large deviations exist even after data smoothing.

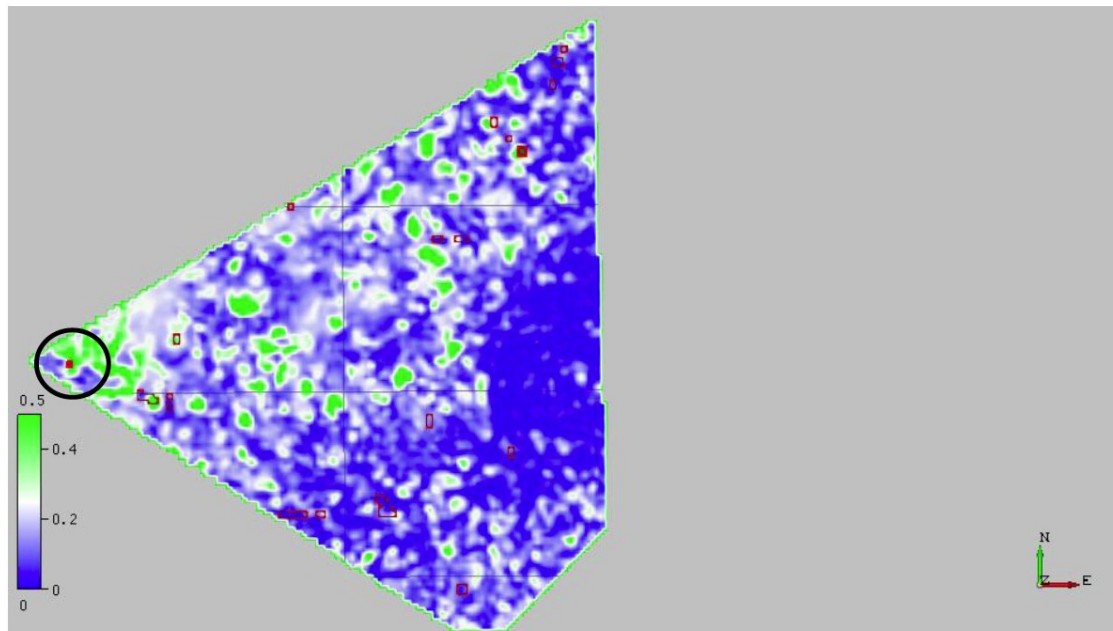


Figure 4: A depth slice showing the predicted permeability and the training points (open red squares). The solid red square with a circle shows a point where the predicted permeability matches the observed permeability.

2.1.2 Model run

Four sets individual models (runs) were used as the final comparison after extensive testing and development. Each run was tested on the eight different training sets to yield a total of 32 runs for each set of software (self-developed and commercial). Both the self-developed and commercial algorithm produced similar results but differed in details. The difference is likely due to differences in implementation. Both implementations were capable of finding relationships that were effective on the training data, but produced false positives when applied to the full dataset. Figure 5 shows the generalized process. Once the training run was complete, the resulting model was tested on a set of known points that were not used in the training dataset. For the training runs, several runs produced correlation of over 0.9, which is considered good.

The first run used a set of selected seismic attributes that had been shown in the previous work to show correlation with the permeability. This was based largely on cross plots of permeability index versus attribute. After calibrating the neural network with the training data, the overall fits to permeability along the entire well bore were quite low. The type II input dataset worked slightly better for the Optim algorithm but showed no change for the Petrel algorithm. The second run included information from mineralogy along the well bore. This showed no clear improvement over only attributes, possibly due to inadequately sampled data or little correlation between permeability and mineralogy. The third run included information from facies and lithology as well as the attributes. This yielded an overall improvement in results. Permeability prediction improved, possibly due to the known enhancement of permeability in the Elba quartzite. The fourth model, which combined all information provided the best overall results (Figure 6) but difficult to interpret the underlying reasons due to the complexity of input.

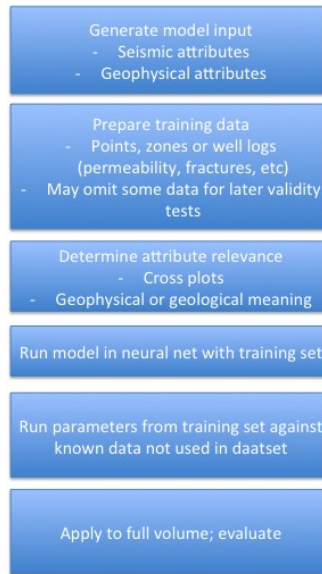


Figure 5: Flow chart showing processing steps for attributes analysis.

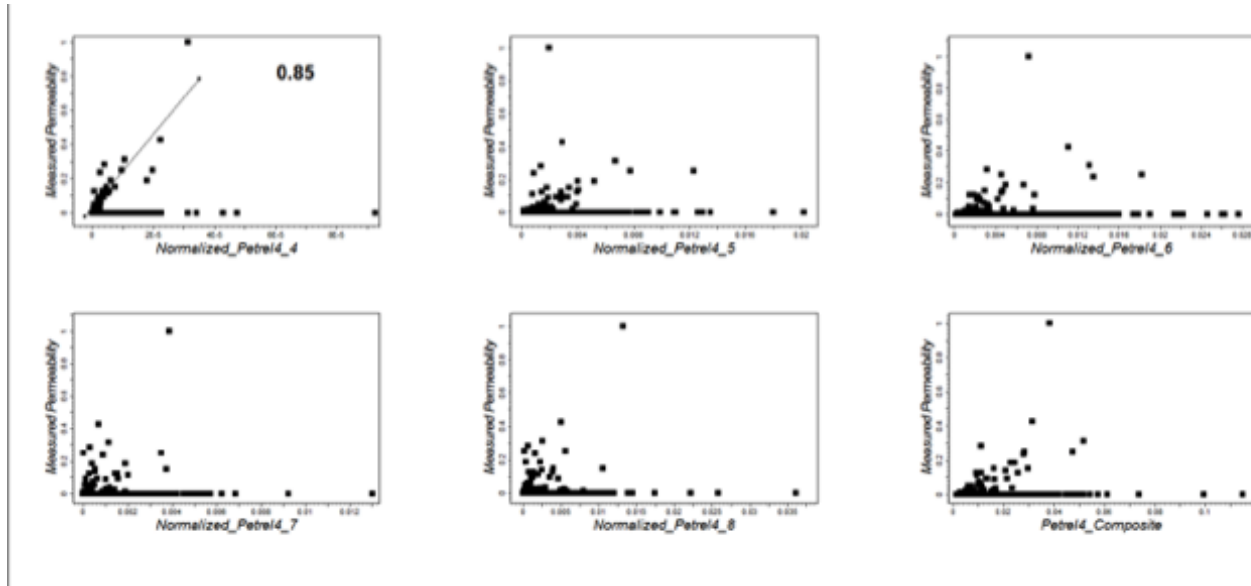


Figure 6: Example of output from run #4 for each of the permeability classifications and the composite model. Model #4 displayed the higher correlation between permeability and the input data. The vertical axis is permeability and horizontal is the samples.

2.2 Micro-earthquakes and reflection seismic

Another use of the 3D data is to use the amplitude images to examine structure. In particular, it is of interest to see if the microearthquake locations correspond to clear structural features in the 3D seismic data. Using hypocenters (x,y, and z) from the LBL catalog (http://esd1.lbl.gov/research/projects/induced_seismicity/egs/raft_river.html), the microearthquakes (MEQ) were plotted on the depth migrated seismic reflection data.

MEQ were plotted on series of horizontal and vertical slices (Figures 7, 8, 9 and 10). The basement interface is visible as a strong reflector and it is clear that MEQ occur below the reflector. Horizontal slices ate the interface and in the basement show complexity and indications of compartmentalization but again not features that match directly with the microseismicity. Although the MEQ appear to occur along a roughly linear fashion, no obvious single discontinuity is visible in the horizontal section. The vertical sections show some slightly discontinuous features that might be faults cutting the section at high angle, but a single distinct feature is not obvious. This result is slightly surprising and indicate that seismogenic faults are challenging to identify in geothermal areas using reflection seismic data.

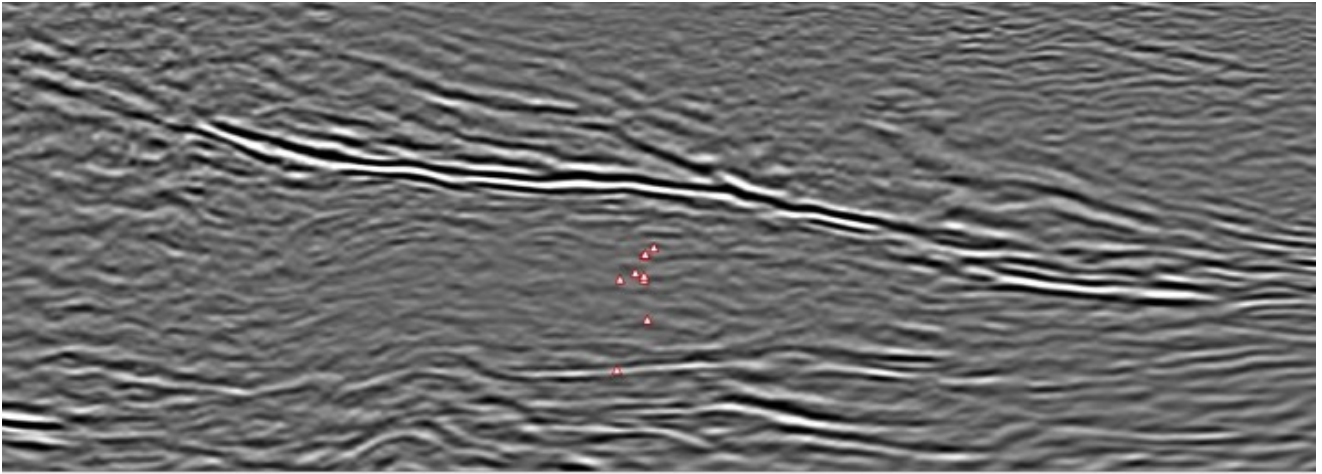


Figure 7: Vertical slice, with MEQ within 250 feet shown.

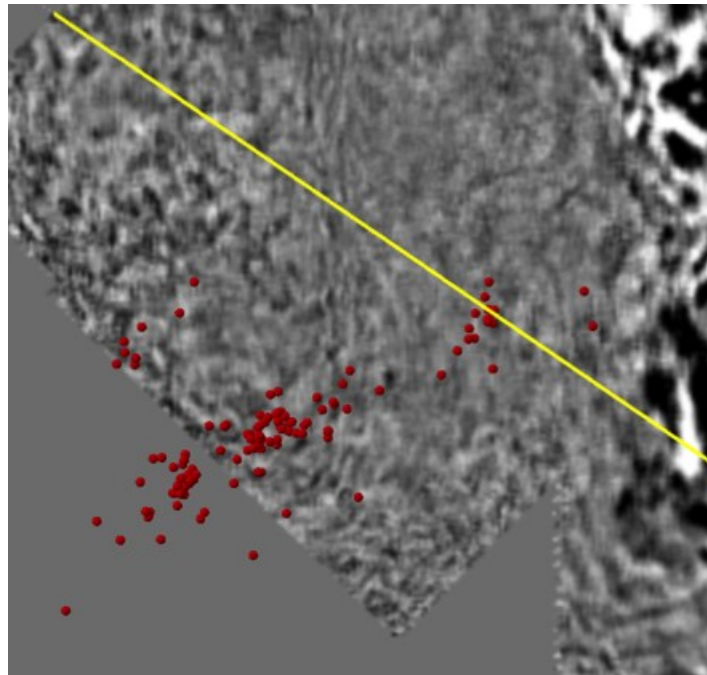


Figure 8: Horizontal slice, with MEQ within 250 feet shown. Yellow line correspond to section shown in Figure 7.

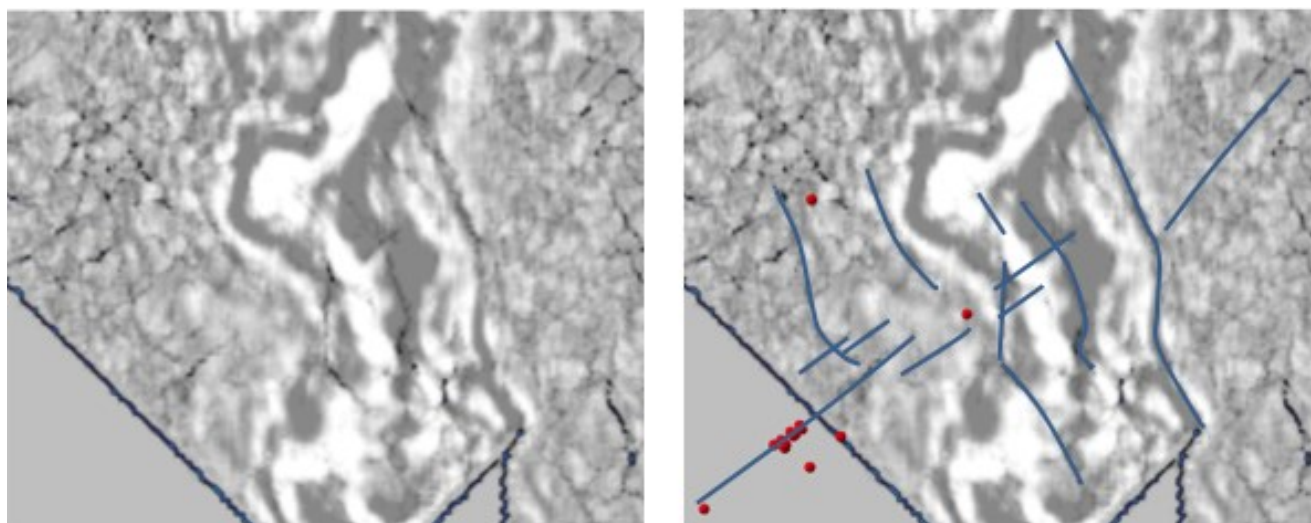


Figure 9: Horizontal slice showing amplitude view of the basement (left) with micro-earthquakes and interpreted ant-tracked lineaments shown (right). This slice cuts through the east-dipping Elba/basement contact.

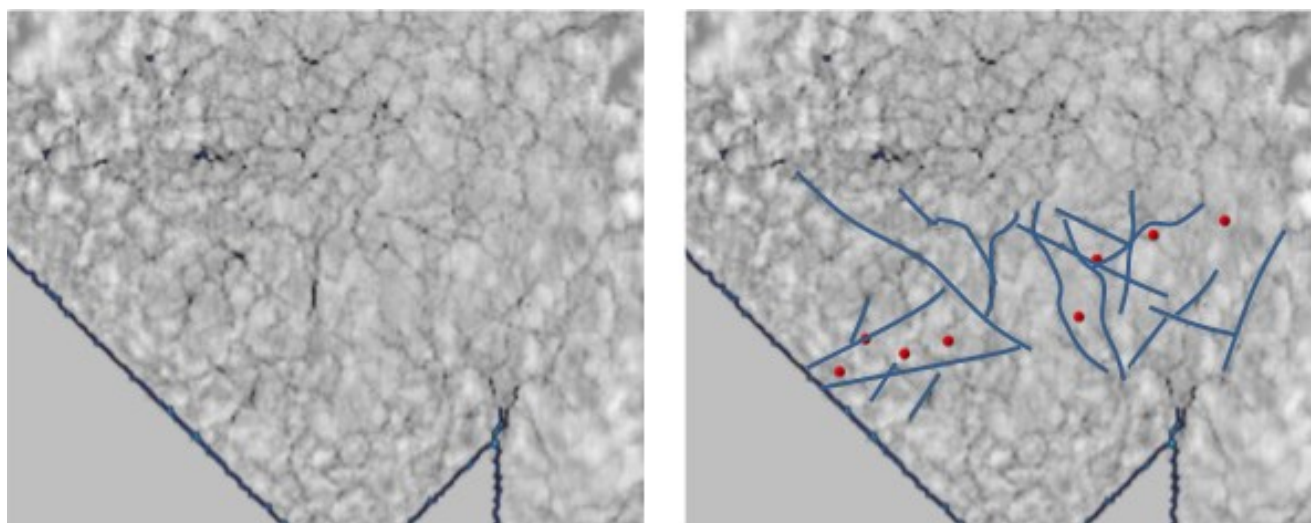


Figure 10: Horizontal slice showing an edge enhanced view of the basement (left) with micro-earthquakes and interpreted ant-tracked lineaments shown (right). The slice is located well below the Elba quartzite.

3. CONCLUSIONS

The neural net analysis indicates that the method is effective at finding relationships between attributes and permeability that are not obvious otherwise, but a clear relationship that matches the geology and is effective at predicting permeability has not yet been discovered. Achieving a high correlation for a training set is possible, but tends to yield a large number of false positives when applied to real data. It is clearly possible to identify zones of faults and complexity, but not all faults are permeable. The addition of mineralogical data did not improve results. Structurally derived data tended to influence results, but not always as an improvement. Lithological data did improve results significantly. Given the inherent risks, it proved not possible to locate a new ell based on these data alone.

Ultimately, the success of permeability mapping efforts hinges on the input data against which the training datasets are modeled. It is these seismic attributes (or geological or spatial properties) that drive the results, and while the neural net modeling can derive a function to describe where permeability exists at measured locations, it struggles to adequately describe (due to lack of an adequate attribute?) or set apart non-permeable zones. In simple terms, even a suite of different attributes, and with advanced modeling techniques, is not sufficient for mapping permeability ubiquitously across the field. The conclusion from this is that either/or 1) an attribute with a more robust link to permeability is needed, or 2) the model space needs to be better zoned or segmented and modeled separately such that attributes that work in part of the reservoir are not applied to other areas where they may be less relevant, or worse,

falsely representing the underlying reservoir characteristic; or 3) the seismic data may contain inaccuracies or misrepresentations, which ultimately misleads the modeling efforts. Future efforts will focus on incorporating new attributes (elements of #1), with #2 above, to yield improved results for prioritized target areas. The quality of the seismic data appears good, and we have no direct evidence that is a cause for lack of modeling success. Indeed, it is likely that the modeling would not perform as well as it does on known data points if the seismic data lacked a reasonable and consistent tie to geologic reality.

Examination of microearthquake locations and 3D seismic data show that the earthquakes correlate areas of more complexity but are not obviously associated with clearly defined faults

Acknowledgment. This work was supported by DOE Geothermal Technologies Office. We thank Ernie Majer for providing microseismic information and Joe Moore for useful discussions and mineralogical analysis. Prepared by LLNL under Contract DE-AC52-07NA27344.

REFERENCES

- Verma, A., and Pruess, K.: Enhancement of Steam Phase Relative Permeability Due to Phase Transformation Effects in Porous Media, *Proceedings*, 11th Workshop on Geothermal Reservoir Engineering, Stanford University, Stanford, CA (1986). <Reference Style>
- Barnes, A.: Seismic attributes past, present, and future. SEG Technical Program Expanded Abstracts 1999: pp. 892-895. doi: 10.1190/1.1821230 (1999).
- Barnes, A. Too many seismic attributes? CSEG recorder, <http://csegrecorder.com/articles/view/too-many-seismic-attributes>. (2006)
- Bradford, J., McLennan, J., Moore, J. Glasby, D., Waters, D., Kruwell, R, Bailey, A., Rickard, W., Bloomfield, K, and King, D.: Recent developments at the raft river geothermal field. Proceedings of thirty-eighth workshop on geothermal reservoir engineering; Stanford University: thirty-eighth workshop on geothermal reservoir engineering (2013)
- Brieman, L.: Bagging Predictors, *Machine Learning*, 24(2), (1999) pp. 123-140.
- Broomhead, D.S. and Lowe, D.: Multivariable functional interpolation and adaptive networks, (1988)
- Chopra, S. and Marfurt, K.: Seismic attributes for fault/fracture characterization, SEG/San Antonio 2007 Annual Meeting (2007)
- Drucker, H., Burges, C. J., Kaufman, C., L.Smola, A. J. and Vapnik, V. N.: Support Vector Regression Machines, in *Advances in Neural Information Processing Systems 9*, NIPS 1996, (1997), 155–161, MIT Press.
- Jones, C., Moore, J., Teplow, W. and Craig, S.: Geology and hydrothermal alteration of the Raft River geothermal system, Idaho, Proceedings, Thirty-Sixth Workshop on Geothermal Reservoir Engineering, Stanford University, Stanford, California, January 31 - February 2, 2011
- Louie J. N., Pullammanappallil, S. K., and Honjas, W.: Advanced seismic imaging for geothermal development, (2011)
- Majer, E.: 3-D Seismic Methods for Geothermal Reservoir Exploration and Assessment—Summary, Technical report, DOI: 10.2172/840868 (2003).
- Marfurt, K. J., R. L. Kirlin, S. L. Farmer, and M. S. Bahorich.: 3-D seismic attributes using a semblance-based coherency, (1998)
- Nakagone, O., R. Uchida, and T. Horoikoshi: Seismic reflection and VSP in the Kakkonda geothermal field, Japan: Fractured reservoir characterization, *Geothermics*, 27, (5/6), (1998).
- Neves F. A., Zahrani M. S. and Bremkamp S. W.: Detection of Potential Fractures and Small Faults Using Seismic Attributes,” *The Leading Edge* 23, no. 9 (September 2004): 903–906.
- Reedmilller M., and Heinrich B: Rprop - A Direct Adaptive Method for Faster Backpropagation Learning: The RPROP Algorithm . IEEE International Conference on Neural Networks (1993)., pp. 586–591.
- Specht, D.H.: A General Regression Neural Network, *IEEE Trans Neural Networks*. 1991;2(6):568-76, (1991).
- Unruh, J., S. Pullammanappallil, W. Honjas, and F. Monastero: New seismic imaging of the Coso field, Eastern California, Proceedings of the twenty-second workshop on Geothermal Reservoir Engineering, Stanford University, Stanford, California, (2001).